Available online at www.sciencedirect.com
ScienceDirect
Coordination Chemistry Reviews 251 (2007) 1878–1888
COORDINATION CHEMISTRY REVIEWS
www.elsevier.com/locate/ccr

Review

Using coordination chemistry to develop new routes to semiconductor and other materials☆

Dongbo Fan, Mohammad Afzaal, M. Azad Mallik, Chinh Q. Nguyen, Paul O'Brien*, P. John Thomas

School of Chemistry, The University of Manchester, Oxford Road, Manchester M139PL, UK

Received 11 January 2007; accepted 30 March 2007
Available online 5 April 2007

Contents

Abstract

Recent results from our laboratory on the synthesis of single-source precursor (SSP) molecules and their use for the making nanomaterials by different techniques are presented. The precursors include dichalcogenoimidophosphinate, dialkylchalcogenophosphates, ionic dialkyldiselenophosphinate salts and dithiocarbamates. Solution phase thermal decomposition, chemical vapour deposition (CVD) and interfacial deposition techniques have been used to obtain nanocrystals and thin films of semiconducting material.

Keywords: Single-source precursors (SSP); Nanomaterials; Semiconductors

1. Introduction

The search for new routes to semiconducting material continues to attract considerable attention, despite the many advances that have resulted in the semiconductor-based revolution in electronic devices. The key reason for the sustained interest is that semiconductors as a class of materials remain to some extent poorly understood and significant synthetic challenges posed by the reactive nature of the semiconductors remain to be overcome. Among the class of semiconducting material, nanocrystalline semiconductors: crystallites with at least one of their dimension in nanometric domain are possibly most researched class of present-day materials. Nanomaterials promise to unravel the secrets behind fundamental phenomena at the forefront of chemistry and physics. Further, numerous applications have been envisaged for nanomaterials in physical, chemical and biological sciences. It is no surprise therefore that nanoscience, attracts practitioners from different disciplines. In this context, synthesis route to semiconducting material in general and nanocrystals in

☆ Based on a keynote lecture presented at the 37th International Conference on Coordination Chemistry, 13–18 August 2006, Cape Town, South Africa.

* Corresponding author.
E-mail address: paul.obrien@manchester.ac.uk (P. O'Brien).

0010-8545/$ – see front matter © 2007 Elsevier B.V. All rights reserved.
doi:10.1016/j.ccr.2007.03.021

particular assume significance. This paper is based on a keynote lecture delivered at the 37th ICCC conference in South Africa.

The unique properties of semiconductor nanocrystals are a result of two key effects. The first being quantum confinement—the changes in the electronic structure caused by the confinement of the electronic wavefunction to the dimensions of the particle, which is less than the mean free path of electrons. Quantum confinement, in the case of most semiconductor particles, increases the band gap [1]. The inherent dependence of the degree of quantum confinement on size implies that the electronic properties and thereby other material properties now become a function of the size of a nanoparticle. Remarkably, it leads us to the possibility of being able to engineer band gaps and tailor material properties by simply increasing or decreasing the size of nanoparticles of a particular element or compound. Nanoparticles by virtue of their size also possess a high fraction of surface atoms with the surface fraction falling gradually with increase in size. For example, a nanocrystals with a diameter of 1 nm typically has over 75% of its atoms on its surface [2]. This fraction falls to about 30% when the size is increased to 6 nm and to 15% for 10 nm. Catalysis is a pertinent application that benefits from the increased surface area. The incomplete coordination of the surface atoms results in unsatisfied valences and dangling bonds, which ensure that the surface layer of atoms are highly reactive. The atoms at the surface tend to cause the nanocrystals to fuse together to form larger crystallites. In order to avoid such coalescence and precipitation, the surface atoms are rendered passive by binding them to a capping agent. The capping agents form a ligand shell around a nanocrystal and play the key role of determining the "solubility" of a nanocrystal in a solvent.

We have, for several years, been advocating the use of single-source precursors (SSPs) for the synthesis of thin films and nanocrystals. The use of SSPs provides several key advantages over other routes. For example, the existence of preformed bonds leads to material with lower defects. In the case of thin film deposition by chemical vapour deposition (CVD), conditions of flow and temperature become simpler. It is also possible to carry out deposition with relatively simple installations. Several of the single-source precursors are also air-stable and are therefore easier to handle and characterize. Spurred by the success of the use of SSPs and motivated by their potential to reduce the environmental impact of material processing, we have been keenly interested in investigation new routes to difficult to prepare SSPs. In this article, we shall briefly review the recent advances we have made in the easy synthesis of a family of SSPs and their use for synthesis of semiconducting material in the form of thin films and semiconductors by conventional and novel deposition techniques.

2. Some single-molecular systems for semiconductor deposition

2.1. Dichalcogenoimidophosphinate ([N(PR2E)2M])

Imidodiphosphinic acid derivatives $R_2P(E)NH(E)PR'_2$ (R, $R' = CH_3$, C_6H_5; E = O, S, NH) were first prepared by Schmidpeter et al. [3]. The synthetic process has seen been adapted and improved by others to make a wide range of derivatives with R, $R' = {}^{i}Pr$, ${}^{t}Bu$, Et, OEt, OPh and E = S, Se [4–11]. A typical synthesis involves two steps: a simple condensation reaction of R_2PCl with $NH(SiMe_3)_2$ to give the phosphorous(III) compound, followed by oxidation with O, S or Se to give the desired product (see Eqs. (2.1) and (2.2)).

$$2R_2PCl + NH(SiMe_3)_2 \rightarrow R_2PNHPR_2 \quad (2.1)$$

$$R_2PNHPR_2 \xrightarrow{E=O,S,Se} R_2P(E)NHP(E)R_2 \quad (2.2)$$

By deprotonation of the amine H–N bond, the $R_2P(E)NH(E)PR_2$ derivative can be transformed to a bidentate chelating ligand that can form neutral complexes of the type $M[N(R_2PE)_2]_n$ with transition as well as main group metals.

It was not possible to prepare the tellurium analogue of $R_2P(E)NH(E)PR_2$ by oxidizing R_2PNHPR_2 with tellurium, following the scheme outlined in Eqs. (2.1) and (2.2) [12]. Therefore, Chivers and co-workers have recently developed a new scheme, in which R_2PNHPR_2 is first metalated by NaH to form $Na[R_2PNPR_2]$ followed by a reaction with tellurium powder in hot toluene in the presence of *N*,*N*,*N*′,*N*′-tetramethylethylenediamine [13–15]. The as-produced ligand, $Na[N(TePPr^{i}_2)_2]$, when reacting with appropriate metal halide produce complexes $M[N(TeP^{i}Pr_2)]_n$ with a range of metals including Zn, Cd, Hg, Sb, Bi [16].

2.2. Dialkylchalcogenophosphates

Dialkyldiselenophosphates ligands were first developed by Kudchadker et al. [17]. The coordination chemistry of the ligands was investigated with the synthesis and study of spectral properties of several (*O*,*O*′-diethyldiselenophosphato) metals [18–20]. Recently, Liu and co-workers have reported a range of cluster compounds incorporating dialkyldiselenophosphate ligands [21–26]. Diselenophosphonate ligands were prepared by reaction of "woollins reagent" $(PhPSe_2)_2$ with RONa in ROH, which involve cleavage of the four membered ring P_2Se_2 [9].

In the case of dichalcogenophosphinate complexes, sulfur derivatives have been investigated extensively [27–33] while studies on the seleno analogue are limited due to the difficulty of the synthesis process. The first synthesis of diselenonophosphinate ligand and complexes were reported by Kuchen et al. [34–36]. The synthesis process started with the reaction of R_2PCl with Se powder to initially form $R_2P(Se)Cl$ follow by treatment with NaSeH to yield $[R_2PSe_2]Na$ ligand, which reacted further with metal salts to form diselenophosphinate complexes (Scheme 2.1). Following same method, Mueller was able to synthesis and study vibration spectroscopic properties of diphenyldiselenophosphinato complexes of Ni, Co, Cd, Zn, Hg, and Bi [37,38]. However, this synthesis method has the drawback of using highly toxic H_2Se gas in the process of making

$$R_2PCl \xrightarrow{Se} R_2P(Se)Cl \xrightarrow{NaSeH} R_2P(Se)SeNa \xrightarrow{M^{n+}} [(R_2PSe_2)nM]$$

Scheme 2.1.

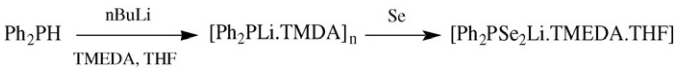

Scheme 2.2.

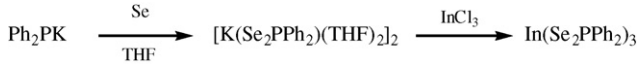

Scheme 2.3.

NaSeH. Using a slightly different route, Pilkington was successful in structurally characterizing a diselenophosphinato complex $Na_2[Ph_2PSe_2]_2$-THF·$5H_2O$ for the very first time [39]. The complex was prepared by reaction of Ph_2PCl with the mixture of Na and Se in liquid NH_3 at −78 °C. This synthetic scheme is however, not reproducible. Recently, Davies et al. have developed a new method for making diselenophosphinate of lithium [40] and potassium [41]. Using the above, indium diselenophosphinato complex was made by exchange ion with potassium complex [41] (Schemes 2.2 and 2.3).

During our attempts to synthesize imido-bis(diisopropylphosphine selenide) ligands, following Woollins method, a mixture of $^{i}Pr_2P(Se)NHP(Se)^{i}Pr$ and $(^{i}Pr_2PSe)_2Se$ were obtained at mild reaction conditions (low concentration, low temperature). The ligand, $(^{i}Pr_2PSe)_2Se$, which was serendipitously formed exhibited interesting coordination properties when reacted with metal salts. In the reaction process, the P–Se bonds are broken to form $^{i}Pr_2PSe_2$ units, which could act as bidentate chelating ligands to form complexes with metal ions. Mindful of the potential use of diselenophosphinato complexes as SSPs, we tried to improve the product yield. However, despite numerous attempts, the yield could not be improved beyond 10%.

In order to find a suitable alternative synthetic method for obtaining the above ligands, the reaction mechanism was investigated. The reaction mechanism for the formation of $^{i}Pr_2P(Se)NHP(Se)^{i}Pr$ has been established and includes the forming of an intermediate R_2PNHPR_2 followed by oxidation with elemental selenium (Scheme 2.4). The mechanism for the by-product may be proposed as forming an intermediate $R_2PSi(Me)_3$ in the first step, followed by inserting Se into the P–Si bond (Scheme 2.5). This proposed mechanism is backed by the study of Horn and Lindner, who have prepared $(Ph_2P(Se)SeP(Se)Ph_2)$ by reaction of Se with $Ph_2PSi(Me)_3$ [42].

It is clear that the diselenophosphinate ligand $(R_2PSe)_2Se$ can be prepared by inserting Se into P–Si of R_2PSiR'. The efficiency of the synthesis relies on the process of making R_2PSiR'. This compound can be prepared by reaction of lithium with R_2PCl to

Scheme 2.4.

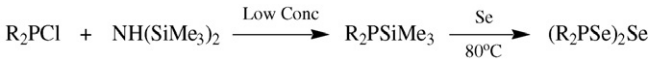

Scheme 2.5.

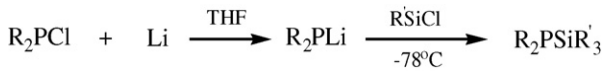

Scheme 2.6.

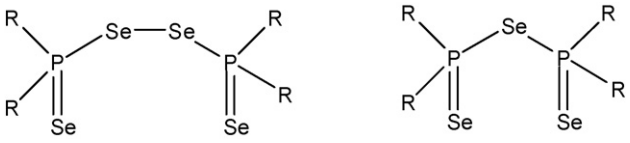

Fig. 1. Structure of $(R_2PSe)_2Se$ and $(R_2PSe)_2Se_2$; (R = ^{i}Pr, Ph).

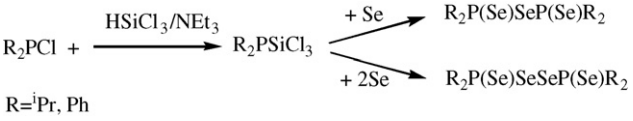

Scheme 2.7.

form R_2PLi, follow by exchange reaction between R_2PLi with R'_3SiCl at low temperature (Scheme 2.6) [43]. The disadvantage of this process is the extreme reaction conditions. Utilising Benkeser reaction [44–46], a similar moiety (R_2PSiCl_3) can be easily prepared with high yield at normal reaction conditions (Eq. (2.3)).

$$R_2PCl + HSiCl_3 + NEt_3 \rightarrow R_2PSiCl_3 + (HNEt_3)Cl \quad (2.3)$$

Based on the discussion above scheme, we have developed a new facile method for making dialkyldiselenophosphinate ligands (Fig. 1). The synthesis process includes two steps: (a) making R_2PSiCl_3 intermediate by the reaction of R_2PCl with $HSiCl_3$ and NEt_3 in toluene under N_2 at room temperature, followed by (b) inserting Se into the P–Si bond of the intermediate by refluxing the intermediate with Se powder in toluene. In step (b), by controlling the Se:R_2PSiCl_3 ratio, two different products can be prepared (Scheme 2.7) [47].

2.3. Ionic dialkyldiselenophosphinate salts

Further investigations on diselenophosphinate ligands have led to new reaction pathways. With the notation that $(R_2PSe_2)^-$ anion may be stabilized, and crystallized as an ionic compound if there is enough counter cation in reaction solution, an excess amount of $HSiCl_3/NEt_3$ was used. However, $HSiCl_3$ reacts readily with NEt_3 to form $(HNEt_3)(SiCl_3)$ as a precipitate, making Se insertion difficult. The use of $HSiEt_3$ instead of $HSiCl_3$ overcome this problem and yields the ionic compound $(HNEt_3^+)(R_2PSe_2^-)$ (Fig. 2). The synthesis process is

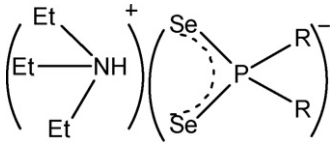

Fig. 2. Structure of $(HNEt_3^+)(R_2PSe_2^-)$; (R = ^{i}Pr, Ph, ^{t}Bu).

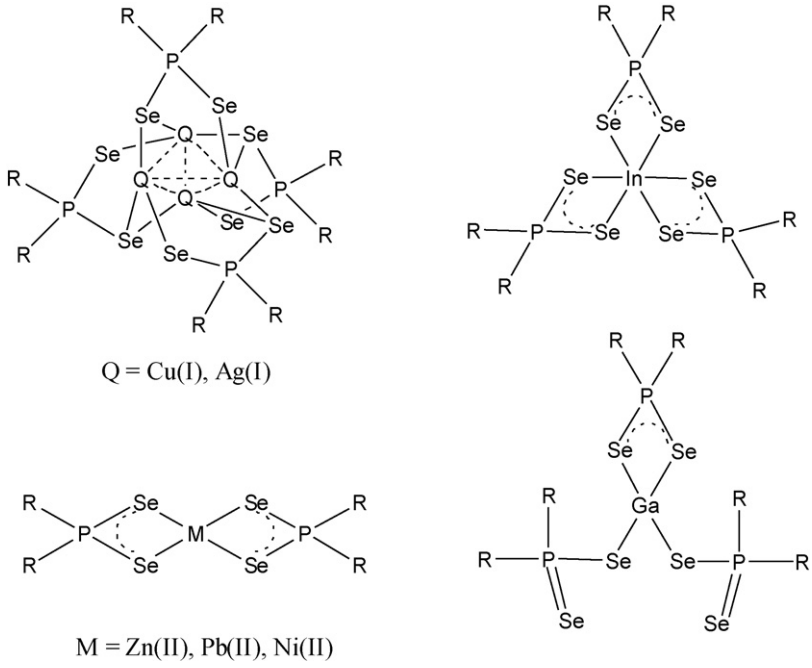

Fig. 3. Structure of some dialkyldiselenophosphinato complexes (R = ^{i}Pr, Ph, ^{t}Bu).

represented in Eq. (2.4).

$$R_2PCl + 2HSiEt_3 + 2NEt_3 \xrightarrow[\text{Toluene}]{\text{Se}} (R_2PSe_2)(HNEt_3) + ClHNEt_3 + Si_2Et_6$$
$$R = {}^{i}Pr; {}^{t}Bu; Ph \quad (2.4)$$

Three ionic ligands (R = ^{i}Pr, ^{t}Bu, Ph) were synthesised with high yield (>80%) by this new method [48]. All three compounds are air-stable and are soluble in most common organic solvents. The X-ray crystal structure of isopropyl derivative indicates that it crystallizes as an ionic salt species, composed of the anion $(^{i}Pr_2PSe_2)^{-}$ and the cation $(Et_3NH)^{+}$.

The reactions of p-block and d-block metal ions with $(^{i}Pr_2PSe)_2Se$ lead to formation of air-stable, inorganic complexes (Fig. 3). During the reaction, one P–Se bond is broken within $(^{i}Pr_2PSe)_2Se$ and this moiety then acts as a source of dialkylselenophosphinate $(R_2PSe_2)^{-}$ [49]. All the compounds are obtained in good yields as crystalline solids by recrystallization from organic solvents.

2.4. Dithiocarbamates

Bis(dialkyldithio-/diseleno-carbamato)cadmium(II)/zinc(II) compounds are prepared by reacting CS_2 or CSe_2 with excess alkylamine and NaOH or KOH at low temperatures, followed by a reaction with zinc or cadmium chloride. The dithiocarbamtes are readily obtained in high yields. The precursors we have explored include those with symmetric alkyl groups (R = R′ = Me, Et, Pr, Pr^{i}) or asymmetric R groups such as R = Me or Et, R′ = ^{n}Hex, ^{n}Bu.

3. Routes from molecules to materials

We have explored the use of several conventional and non-conventional routes for the exploitation of inorganic complexes as single-source precursors. The routes include solution phase thermal decomposition, chemical vapour deposition and deposition at the interface of water–toluene.

3.1. Solution phase thermal decomposition

Nanocrystals are obtained by carrying out the decomposition by injecting a solution of the SSPs into a hot solvent (at temperatures over 200 °C), typically a mixture of tri-*n*-octylphosphineoxide (TOPO) and long chain alkylamine such as hexadecylamine (HDA), followed by refluxing for a specific period of time. The particles are isolated by precipitating the mixture with ethanol or methanol. The diameters of the obtained nanocrystals are dependent on the reaction time, temperature, the ratio of the capping agent and the precursor employed. By varying the conditions employed during synthesis, CdS and CdSe nanocrystals with sizes in the range of 5–6 nm and ZnSe nanocrystals in the size range of 3.5–4.5 nm were obtained starting with dichalcogenocarbamates [50]. From the electronic absorption spectra, it is possible to infer that the obtained nanocrystals possess a higher band gap than the corresponding bulk. The band gaps for ZnSe nanocrystals were in the range of 3.42–3.59 eV (bulk: 2.58 eV), while in the case of CdSe nanocrystals, the band gaps were between 2.02 and 2.09 eV (bulk: 1.73 eV). The observed increase in band gap for CdS nanocrystals was ~0.1 eV. The alkyl chains present in the precursor play a role in determining the products of the decomposition

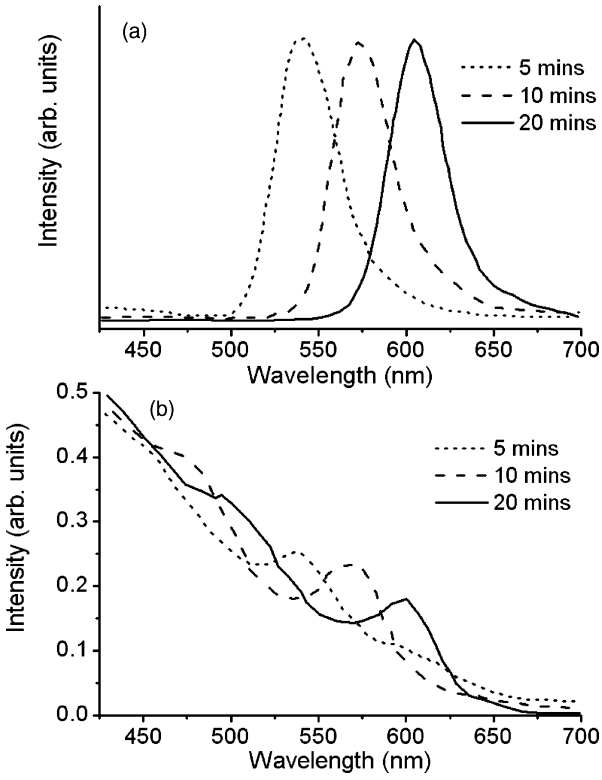

Fig. 4. (a) PL spectra of CdSe QDs at various time intervals, (b) UV–vis spectra of CdSe QDs at various time intervals (reproduced with permission from Ref. [53]).

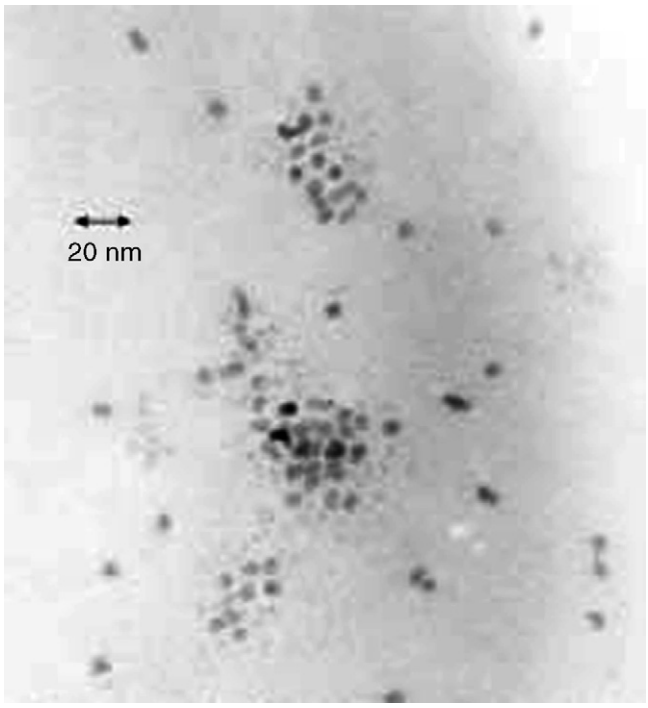

Fig. 5. TEM micrographs of CdSe QDs isolated after 30 min reaction time (reproduced with permission from Ref. [53]).

reaction. In the case of diseleno carbamates, precursors with unsymmetrical R groups such as $Cd(Se_2CNMe^nHex)_2$, yield stoichiometric nanocrystals, while those with symmetrical R groups yield Se clusters and/or Se rich particulates [51]. The dithio precursors, on the other hand, exhibit no such preference. In addition to the dithio and diseleno carbamates, ZnSe nanoparticles with higher diameters have been obtained by the use of ethyl(diethyldiselenocarbamato)zinc(II), $EtZnSe_2CNEt_2$ [52]. As expected, these nanocrystals exhibit a smaller increase in band gap (~0.25 eV).

CdSe nanocrystals capped with HDA have been obtained by thermal decomposition of $Cd[N(SeP^iPr_2)_2]_2$ [53]. Absorption spectra reveal a blue-shifted band edge that shifts to higher energies upon increasing growth time, indicating that nanocrystals of larger diameters are obtained upon increasing growth time. Relative to the bulk band edge (716 nm, 1.73 eV), absorption edge shifts of 0.35, 0.31 and 0.23 eV are observed for nanocrystals isolated after 5, 10 and 20 min, respectively (see Fig. 4a). The as prepared nanocrystals exhibit size-dependent emission in the visible region (see Fig. 4b). Transmission electron microscopic images reveal that the CdSe nanoparticles obtained are spherical and monodisperse with diameters of ~6.0 nm (see Fig. 5).

In addition to II–VI material, it has also been possible to extend the synthetic scheme to prepare other groups of semiconductors as well. Nanocrystals of IV–VI material such as PbS and PbSe have been prepared by starting with lead dithio and diseleno carbamates [54]. PbS nanocrystals prepared by decomposition of $Pb(S_2CN^iBu_2)_2$ exhibit different morphologies, based on the temperature employed for the preparation. The nanocrystals synthesized at 100 °C were spherical with average diameters of 6.3 nm. At 150 °C, a mixture consisting of a large fraction of cubic crystallites with average size ~60 nm and a small fraction of spherical nanocrystals was obtained (see TEM image Fig. 6). Much larger cubes were obtained by the decomposition of $Pb(S_2CNEt_2)$ at 250 °C (see TEM image in Fig. 7). Similarly, by the use of $Pb(Se_2CNMe^nHex)_2$, PbSe nanocrystals with cubic shape have been obtained. In general, the synthetic schemes that are successful in producing semiconductor nanocrystals of various groups are not readily

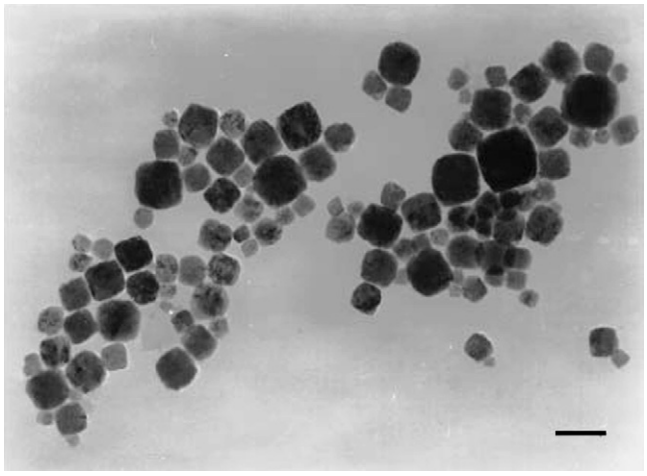

Fig. 6. TEM image of PbS nanocrystals prepared by thermolysis of $Pb(S_2CN^tBu_2)_2$ in TOPO at 150 °C (scale bar = 100 nm) (reproduced with permission from Ref. [54]).

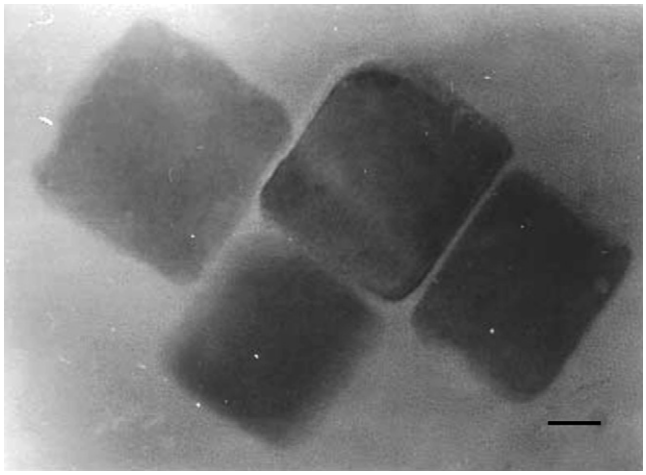

Fig. 7. TEM image of PbS nanocrystals prepared by thermolysis of $Pb(S_2CNEt_2)_2$ in TOPO at 250 °C (scale bar = 100 nm) (reproduced with permission from Ref. [54]).

extendable to produce III–V material, owing to the limitations posed by the increased covalency. However, it has been possible to extend the single-molecule precursor synthesis scheme for the preparation of these nanocrystals as well. By prolonged reflux of indium/gallium diorganophosphide compounds, $M(P^tBu_2)_3$ (M = Ga, In) in 4-ethylpyridine, nanocrystals of GaP and InP exhibiting quantum confinement have been obtained [55]. The InP nanocrystals possessed an average diameter of 7.2 nm (see Fig. 8). The band gap estimated from absorption edge was 1.92 eV (bulk: 1.27 eV). Nanocrystals of II–V material Cd_3P_2 have been obtained by using $[MeCd(P^tBu_2)]_3$ in TOPO and $[MeCd(\mu\text{-}PPh_2)]_3$ $(HPPh_2)_2$ in 4-ethylpyndine [55]. The Cd_3P_2 nanocrystals show marked changes in band gap due to the large bulk exciton diameter. The Cd_3P_2 nanocrystals were slightly elongated with diameters of 5.0 and 4.0 nm and possess band gap of 2.6 and 2.4 eV, respectively (see HRTEM images in Fig. 9). Nanoparticles of III–VI material, InS and InSe, have been prepared using single-molecule precursors $In(E_2CNEt_2)_3$ (E = S or Se) and $In(Se_2CNMe^nHex)_3$ [56–58]. In addition to nanocrystals of binary semiconductors, nanocrystals of ternary semiconducting material such as $CuInSe_2$ could be prepared by using a mixture of $In(Se_2CNMe^nHex)_3$ and $Cu(Se_2CNMe^nHex)_2$ [59]. The diameters of $CuInSe_2$ nanocrystals were ~4.5 nm. The nanocrystals exhibit a large blue shift of 1.95 eV in the absorption edge compared to the bulk and exhibit luminescence (see TEM images and the optical spectra in Fig. 10).

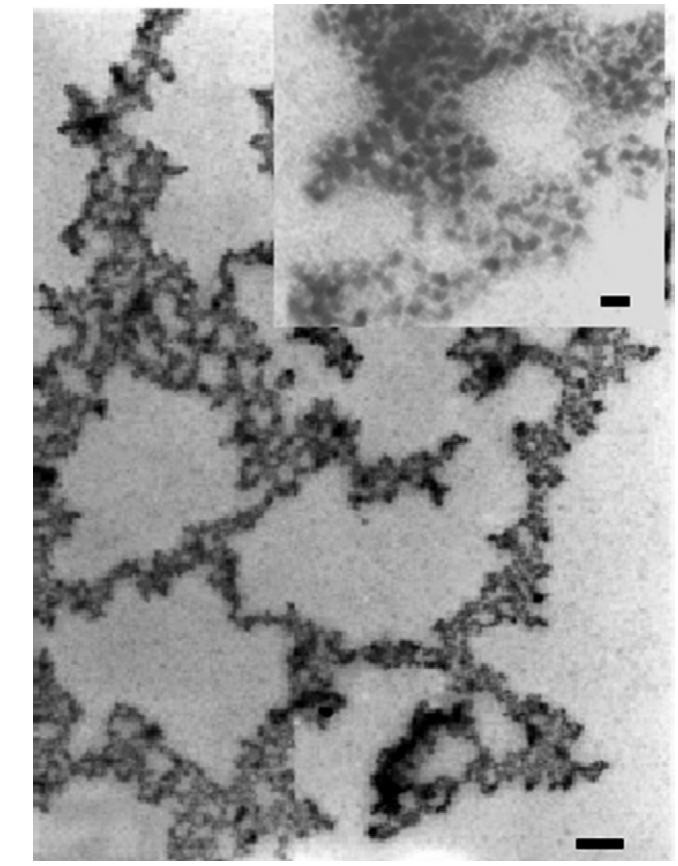

Fig. 8. TEM image of InP nanocrystals (scale bar = 200 nm). The inset shows a higher resolution image of InP nanocrystals showing individual nanocrystals (scale bar = 20 nm) (reproduced with permission from Ref. [55]).

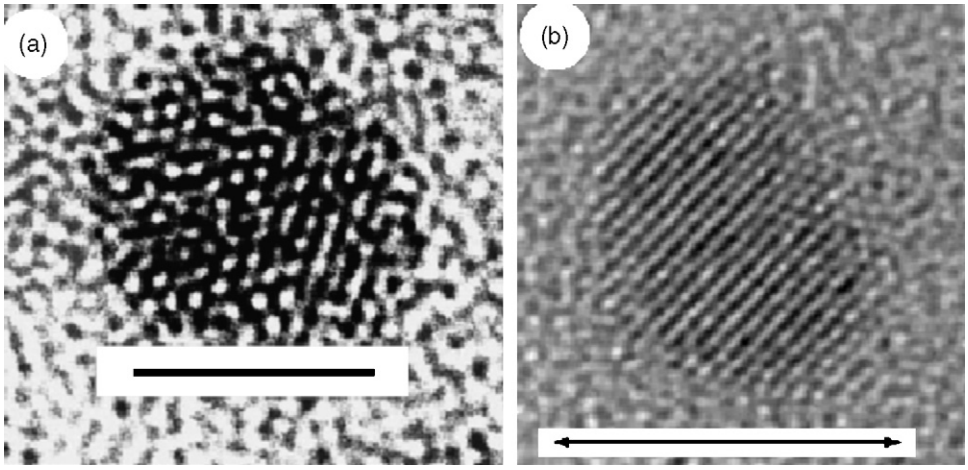

Fig. 9. HRTEM images of: (a) 4-ethylpyridine capped Cd_3P_2 nanocrystals (scale bar = 3 nm); (b) TOPO capped Cd_3P_2 nanocrystals (scale bar = 5 nm) (reproduced with permission from Ref. [55]).

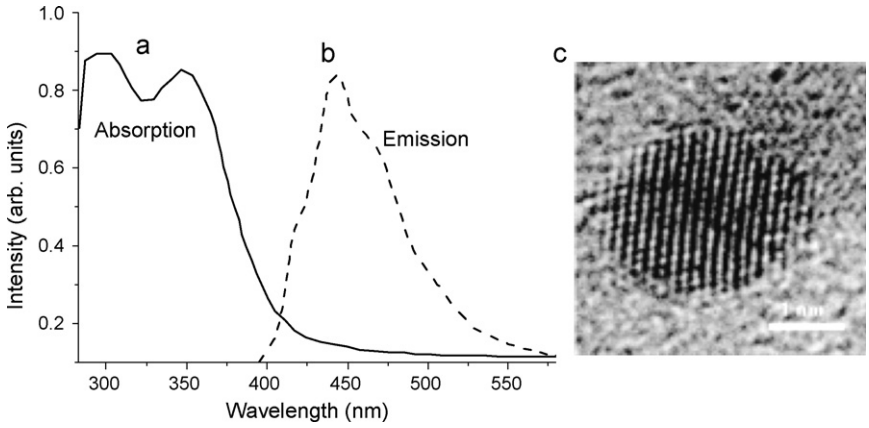

Fig. 10. (a) Optical absorption spectrum of $CuInSe_2$ showing a band edge at 420 nm and an excitonic peak at 352 nm. (b) Photoluminescence spectrum showing an emission at 440 nm. (c) HRTEM image of a single quantum dot of $CuInSe_2$ (ca. 4 nm in diameter) (reproduced with permission from Ref. [59]).

3.2. Synthesis of thin films at the water–toluene interface

The interface between different phases of matter has been put to various uses in the past. The Langmuir–Blodgett technique for deposition of thin films at an air–liquid interface is perhaps best known. There have been several recent reports on the deposition of nanocrystals and thin films at the interface of two immiscible liquids [60]. In this method, a metal precursor dissolved in an organic solvent such as toluene is held in contact with an aqueous layer containing, for example, a reducing agent, sulfiding agent or base. The reaction (reduction, sulfidation or hydrolysis) proceeds via the ion transport mediated at the interface. The products of these reactions are deposited at the interface typically forming thin films or aggregates of nanocrystals. The macroscopic structure of the deposit at the interface is reflective of the structure of the interface. The interface, thus, has a dual role of moderating charge/ion transport and directing the structure of the deposit. Such a method of interfacial deposition is emerging as a simple, convenient and inexpensive route to thin films. Films can be deposited at low temperatures and subsequently transferred to a variety of substrates. The thickness and other characteristics of the deposited layers may be controlled by variation of the deposition parameters such as deposition time. The process is potentially easily adapted to large area processing with low fabrication cost.

We have grown freestanding thin films consisting of nanocrystalline CdS using this method [61]. In a typical reaction, cadmium diethyldithiocarbamate in toluene is allowed to stand in contact with an aqueous solution of Na_2S. A yellow deposit forms at the interface of the two liquids over a period of few hours. The aqueous and the organic phases remain colourless throughout. The films are lifted onto a substrate by gently moving it across the interface. X-ray diffraction patterns reveal that the films are polycrystalline with grain sizes less than 10 nm. Investigations by atomic force microscopy, high-resolution transmission electron microscopy and scanning electron microscopy (SEM) reveal the presence of diverse structural features at different length scales in these CdS films. Scanning electron microscopy reveals that the films consist of flaky deposits that form a macroscopically smooth surface at the interface (see Fig. 11). High-resolution transmission electron microscopy on individual flakes reveals that each flake consists of a mosaic of single-crystalline grains with dimensions of ca. 6 nm (Fig. 12). Nano-scalar granules measuring tens of nanometers that adorn the surface are discernible in atomic force microscopic images. These granules presumably are aggregates of single-crystalline grains. Absorption spectrum of a CdS film deposited on glass substrate at various time intervals is shown in Fig. 13. The overall intensity increases with increase in time, reflecting the increased thickness of the films. The extrapolations of the curves to the energy axis for the zero absorption indicate a band gap of 2.53 eV with a defect state at 3.32 eV (Fig. 14). The higher than bulk band gap is indicative of quantum confinement effects and is expected for nanogranular films. It is significant that the band edge remains constant with increase in deposition time (see Fig. 13), indicating that interfacial deposition is brought about by an increase in population of monodispersed nanocrystals rather than by growth of seeds into large grains by aggregation. Following a similar procedure, ZnS can be deposited at the interface by using zinc diethyldithiocar-

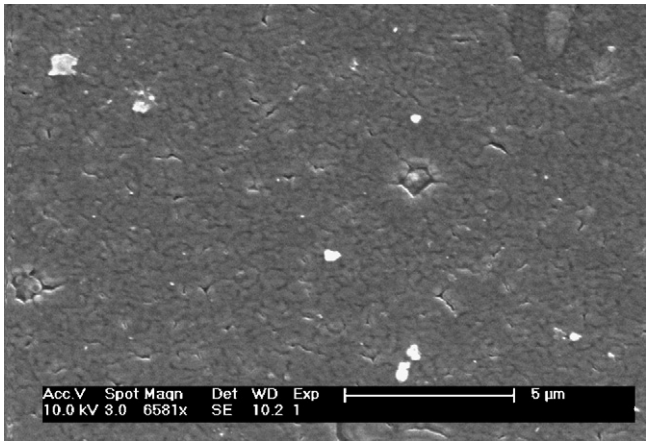

Fig. 11. Scanning electron microscopy (SEM) images of CdS thin films formed by reacting 30 ml toluene solution of 1.67 mM cadmium diethyldithiocarbamate and 30 ml sodium sulfide of 167 mM (reproduced with permission from Ref. [61]).

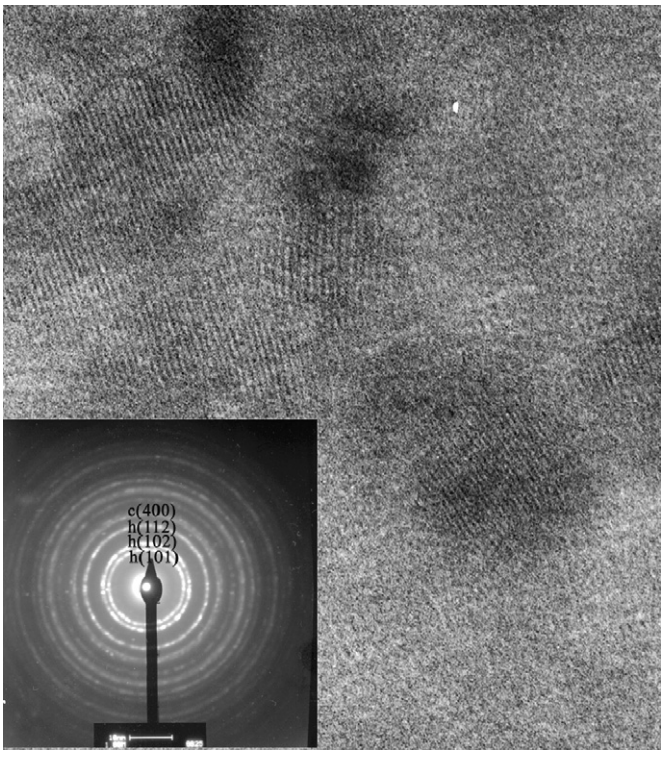

Fig. 12. Transmission electron microscopy image (TEM) and the corresponding SAED pattern of CdS thin film obtained by reacting 30 ml toluene solution of 1.67 mM $Cd(S_2CNEt_2)_2$ and 30 ml Na_2S solution of 1.67 mM at 60 °C for 3 h (reproduced with permission from Ref. [61]).

bamate. X-ray diffraction pattern reveals that the films consist of large micron-sized grains with hexagonal zinc-blende structure. Accordingly, the optical band gap of the films (3.5 eV) is close to the bulk value (3.6 eV). SEM image of ZnS thin film on quartz substrates reveals that the films consist of flakes with dimensions of ∼500 nm (see Fig. 15). It is clear that the growth mechanisms of the ZnS deposits are different from that of CdS.

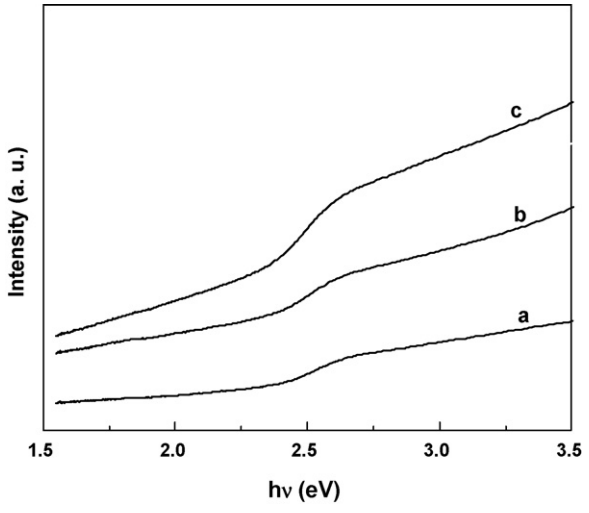

Fig. 13. Uv–vis spectra of CdS films obtained by 30 ml toluene solution of 1.67 mM $Cd(S_2CNEt_2)_2$ and 30 ml Na_2S solution of 1.67 mM at 60 °C for different reaction time: (a) 60 min; (b) 120 min; (c) 180 min (reproduced with permission from Ref. [61]).

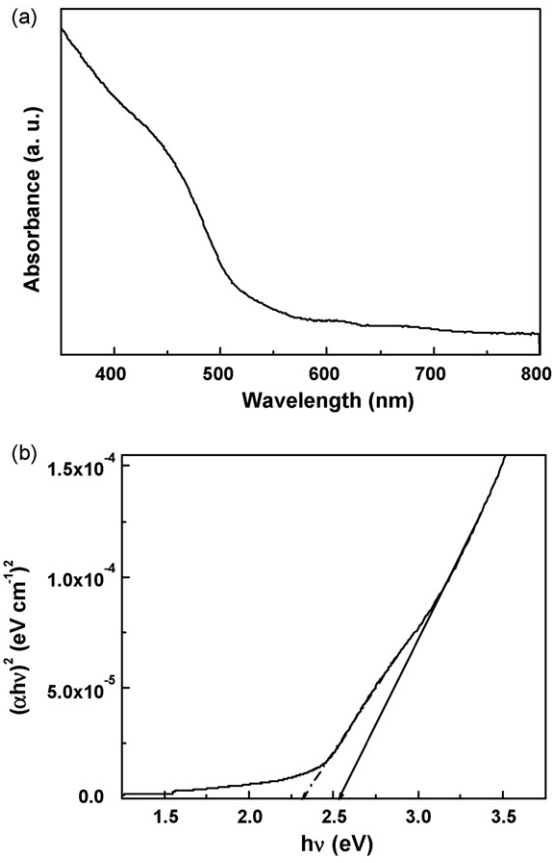

Fig. 14. (a) Electronic absorption spectrum of CdS thin film deposited by using 30 ml toluene solution of 1.67 mM $Cd(S_2CNEt_2)_2$ and 30 ml Na_2S solution of 1.67 mM at 60 °C for 3 h, (b) A plot of $(\alpha h\nu)^2$ vs. $h\nu$ of CdS thin film (reproduced with permission from Ref. [61]).

However, the reason for the difference is not yet apparent. We have been able to extend the interfacial deposition process to other material such as oxides and oxyhydroxides of Co and Ni.

There is little understanding of the interfacial deposition process. The seeds that nucleate the growth of films are adsorbed at the interface due to their ability to act as surfactants. Further work is required to understand the process of interfacial deposition.

3.3. Chemical vapour deposition

The various precursors have been used as chemical sources in the aerosol-assisted chemical vapour deposition (AACVD) process. In this process, a fine mist of the precursor solution is mixed with a carried gas and pyrolysed to in the traditional vapour deposition process to obtain thin films (see schematic illustrated in Fig. 16. By pyrolysis of single-source precursor $Et_2In(S_2CNMe^nBu)$ at 375 °C, nanorods of β-In_2S_3 can be deposited on glass substrates [62]. The obtained nanorods are of ∼20 nm diameter and around 400–500 nm in length (see the electron microscopic images Fig. 17). High-resolution transmission electron microscopy, selected area electron diffraction and X-ray diffraction measurements confirm the crystalline nature of the nanorods. Studies on controlling the diameter of the nanorods by the use of catalyst particle are being undertaken. By employ-

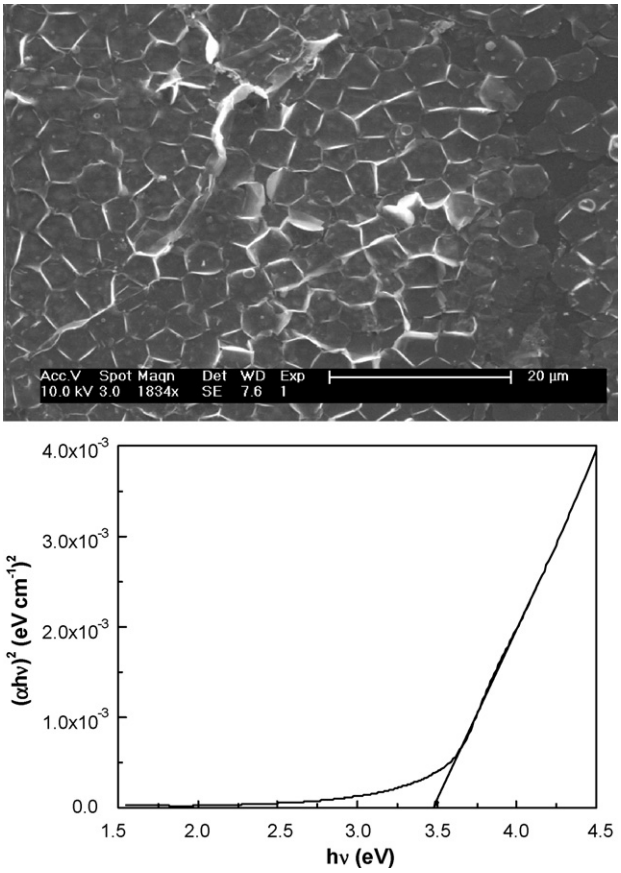

Fig. 15. (Top) Scanning electron microscopy (SEM) image of ZnS thin film deposited by liquid–liquid interface route. (Bottom) A plot $(\alpha h\nu)^2$ vs. $h\nu$ of ZnS thin film (reproduced with permission from Ref. [61]).

ing a slightly modified process, nanorods of PbS have been obtained on Si substrates coated with Au nanocrystals. The imidodiphosphinic acid derivative $M[(TeP^iPr_2)_2N]_2$ (M = Cd, Hg) have been used in aerosol-assisted chemical vapour deposition processes to prepare thin films of chalcogenide material [63].

The cadmium complex yields cubic CdTe films in between when deposition is carried out at temperatures in the range of 425–475 °C. At low deposition temperatures (375 °C), a mixture of hexagonal tellurium and cubic cadmium telluride is

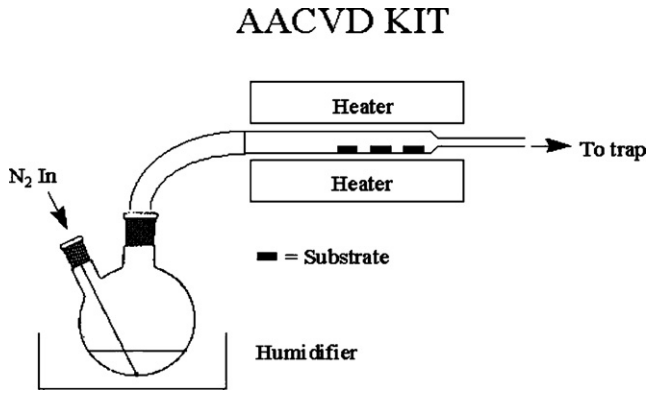

Fig. 16. Schematic illustration of the aerosol-assisted chemical vapour deposition setup.

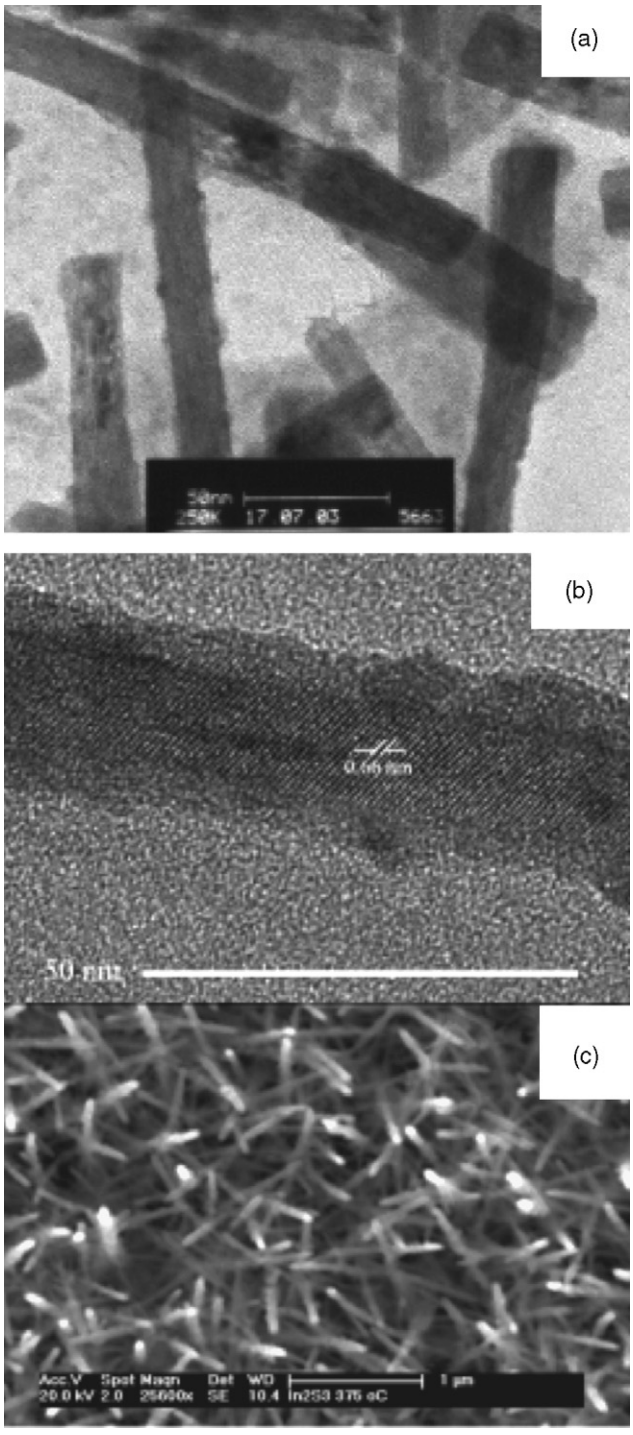

Fig. 17. TEM (a) and HRTEM (b) images of β-In_2S_3 nanowires obtained at 375 °C. (c) SEM image of as grown β-In_2S_3 nanowires on glass substrates (reproduced with permission from Ref. [62]).

obtained (Fig. 18). On the other hand, $Hg[(TeP^iPr_2)_2N]_2$ results in hexagonal tellurium thin films only, possibly due to reductive elimination of mercury at elevated temperatures. It is known that the anionic ligand $[(TeP^iPr_2)_2N]^-$ is readily oxidized to the ditelluride $(TeP^iPr_2N^iPr_2PTe^-)_2$ (which can be viewed as R_2E_2 where $R = Te^iPr_2N^iPr_2P$ and E = Te) [63]. Therefore, reductive elimination of mercury with the concomitant formation of this

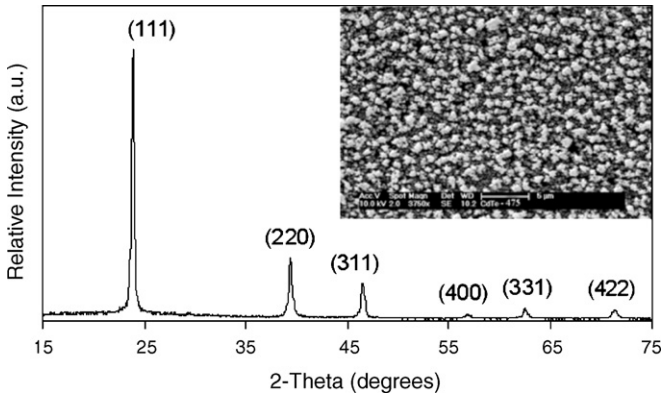

Fig. 18. A typical XRD pattern of cubic CdTe deposited at 475 °C on glass substrate. Inset shows a representative SEM image of the film.

ditelluride is a feasible pathway for the decomposition of precursor. The subsequent degradation of this ditelluride to give hexagonal Te films may account for the current observations.

The usefulness of dialkyldiselenophosphinates compounds as potential single-source precursors were assessed, e.g. by depositing ternary compounds such as copper indium selenide ($CuInSe_2$). Ternary metal chalcogenides such as $CuInSe_2$ have been focus of much recent research due to their use in high efficiency, radiation hard, solar cells. They also have a significant fabrication advantage over III–V semiconductors for solar cell applications, since polycrystalline films may be used, as opposed to epitaxial crystal films [49].

Deposition of $CuInSe_2$ films was carried out by aerosol-assisted chemical vapour deposition [64] using 1:1 molar ratios of $[In(^iPr_2PSe_2)_3]$ and $[(^iPr_2PSe_2)_4Cu_4]$ in 20 ml toluene. The deposition was conducted on glass substrates for 90 min with a dynamic argon flow rate of 120 seem between 400 and 500 °C. Deposited films were black and non-adherent to the substrates. The XRPD analyses (Fig. 19) suggest that deposited films crystallize in the tetragonal phase with a preferred orientation along the (1 1 2) direction in all cases (JCPDS 40-1487). These findings are consistent with the previous studies of $CuInSe_2$ films deposited using dual-source precursors [65]. The SEM image of the films deposited at 400 °C indicates randomly orientated platelets on the glass (Fig. 20). The stoichiometry of films determined by X-ray analysis was close to idea 1:1:2. Traces of phosphorous (ca. 2%) were also detected by the spectra.

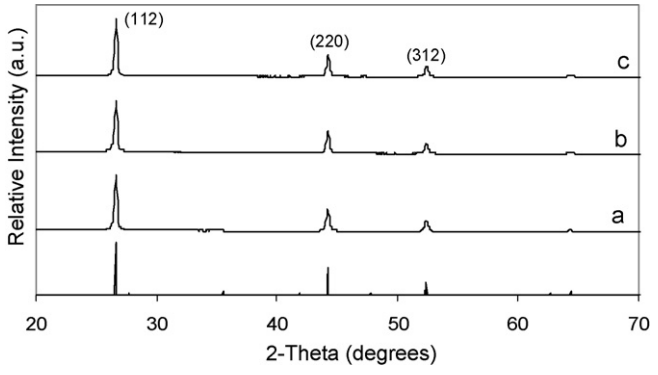

Fig. 19. XRD pattern of $CuInSe_2$ films grown at: (a) 400 °C, (b) 450 °C and (c) 500 °C. The standard pattern for tetragonal $CuInSe_2$ (JCPDS 40-1487) is shown for comparison (reproduced with permission from Ref. [64]).

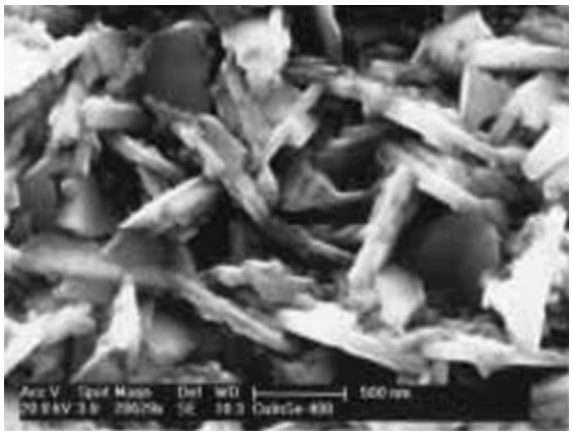

Fig. 20. SEM image of $CuInSe_2$ film deposited at 400 °C (reproduced with permission from Ref. [64]).

4. Conclusions

New synthetic schemes to inorganic complexes that can act as single-source precursors have been described. We have shown how families of single-source precursors can be used for the synthesis of different forms of materials ranging from freely dispersed nanocrystals, thin films and nanorods adhered to substrates. The synthesis has been made feasible by the properties of the precursors such as their solubility and volatility.

Acknowledgements

We would like to thank EPSRC and the Royal Society for extensive support for POB group. DF thanks ORS for funds. PJT thanks RCUK for support. CQN acknowledges the Government of Vietnam for funding.

References

[1] T. Trindade, P. O'Brien, N.L. Pickett, Chem. Mater. 13 (2001) 3843.
[2] C.N.R. Rao, G.U. Kulkarni, P.J. Thomas, P.P. Edwards, Chem. Eur. J. 8 (2002) 28.
[3] A. Schmidpeter, R. Böhm, M.H. Groeger, Angew. Chem. 76 (1964) 860.
[4] T.F. Wang, J. Najdzionek, K.L. Leneker, H. Wasserman, D.M. Braitsch, Synth. React. Inorg. Met.-Org. Chem. 8 (1978) 119.
[5] D. Cupertino, D.J. Birdsall, A.M.Z. Slawin, J.D. Woollins, Inorg. Chim. Acta 290 (1999) 1.
[6] D. Cupertino, R. Keyte, A.M.Z. Slawin, D.J. Williams, J.D. Woollins, Inorg. Chem. 35 (1996) 2695.
[7] D.J. Birdsall, A.M.Z. Slawin, J.D. Woollins, Polyhedron 20 (2001) 125.
[8] D.C. Cupertino, R.W. Keyte, A.M.Z. Slawin, J.D. Woollins, Polyhedron 18 (1999) 707.
[9] I.P. Gray, A.M.Z. Slawin, J.D. Woollins, Dalton Trans. 12 (2005) 2188.
[10] T.Q. Ly, J.D. Woollins, Coord. Chem. Rev. 176 (1998) 451.
[11] I. Haiduc, in: J.A. McCleverty, T.J. Meyer (Eds.), Comprehensive Coordination Chemistry—II, vol. 1, Elsevier, 2004, p. 323.
[12] P. Bhattacharyya, J.D. Woollins, Polyhedron 14 (1995) 3367.
[13] G.G. Briand, T. Chivers, M. Parvez, Angew. Chem. Int. Ed. 41 (2002) 3468.
[14] T. Chivers, D.J. Eisler, J.S. Ritch, H.M. Tuononen, Angew. Chem. Int. Ed. 44 (2005) 4953.

[15] J. Ellermann, M. Schutz, F.W. Heinemann, M. Moll, Z. Anorg. Allg. Chem. 624 (1998) 257.
[16] T. Chivers, D.J. Eisler, J.S. Ritch, Dalton Trans. 16 (2005) 2675.
[17] M.V. Kudchadker, R.A. Zingaro, K.J. Irgolic, Can. J. Chem. 46 (1968) 1415.
[18] V. Krishnan, R.A. Zingaro, Inorg. Chem. 8 (1969) 2337.
[19] V. Krishnan, R.A. Zingaro, J. Coord. Chem. 1 (1971) 1.
[20] T.S. Lobana, J.-C. Wang, C.W. Liu, Coord. Chem. Rev. 251 (2007) 91.
[21] C.W. Liu, I.J. Shang, C.M. Hung, J.C. Wang, T.C. Keng, J. Chem. Soc., Dalton Trans. 9 (2002) 1974.
[22] C.W. Liu, H.C. Chen, J.C. Wang, T.C. Keng, Chem. Commun. 17 (1998) 1831.
[23] C.W. Liu, T.S. Lobana, B.K. Santra, C.M. Hung, H.Y. Liu, B.J. Liaw, J.C. Wang, Dalton Trans. 4 (2006) 560.
[24] B.K. Santra, C.M. Hung, B.J. Liaw, J.C. Wang, C.W. Liu, Inorg. Chem. 43 (2004) 7570.
[25] C.W. Liu, H.C. Haia, C.M. Hung, B.K. Santra, B.J. Liaw, Z. Lin, J.C. Wang, Inorg. Chem. 43 (2004) 4464.
[26] B.K. Santra, B.J. Liaw, C.M. Hung, C.W. Liu, J.C. Wang, Inorg. Chem. 42 (2003) 8866.
[27] M.A. Malik, C. Byrom, P. O'Brien, M. Motevalli, Inorg. Chim. Acta 338 (2002) 245.
[28] W.E.V. Zyl, J.M. López-de-Luzuriaga, J.P. Fackler Jr., R.J. Staples, Can. J. Chem. 79 (2001) 896.
[29] V. Garcia-Montalvo, A. Marcelo-Polo, R. Montoya, R.A. Toscano, S. Hernandez-Ortega, R. Cea-Olivares, J. Organomet. Chem. 623 (2001) 74.
[30] R.G. Cavell, B. Creed, L. Gelmim, D.J. Law, R. McDonald, A.R. Sanger, A. Somogyvan, Inorg. Chem. 37 (1998) 757.
[31] M.N. Gibbons, D.B. Sowerby, C. Silvestru, I. Haiduc, Polyhedron 15 (1996) 4573.
[32] S.N. Olafsson, T.N. Petersen, P. Andersen, Acta Chem. Scand. 50 (1996) 745.
[33] C.C. Landry, A. Hynes, A.R. Barron, I. Haiduc, C. Silvestru, Polyhedron 15 (1996) 391.
[34] W. Kuchen, J. Metten, A. Judat, Chemische Benchte-Recueil 97 (1964) 2306.
[35] W. Kuchen, B. Knop, Angew. Chem. Int. Ed. 4 (1965) 244.
[36] W. Kuchen, H. Hertel, Angew. Chem. Int. Ed. 8 (1969) 89.
[37] A. Mueller, V.V.K. Rao, P. Christophliemk, J. Inorg. Nucl. Chem. 36 (1974) 472.
[38] A. Mueller, P. Christophliemk, V.V.K. Rao, Chem. Ber. 104 (1971) 1905.
[39] M.J. Pilkington, A.M.Z. Slawin, D.J. Williams, J.D. Woollins, Polyhedron 10 (1991) 2641.
[40] R.P. Davies, M.G. Martinelli, Inorg. Chem. 41 (2002) 348.
[41] R.P. Davies, C.V. Francis, A.P.S. Jurd, M.G. Martinelli, A.J.P. White, D.J. Williams, Inorg. Chem. 43 (2004) 4802.
[42] H.G. Horn, H.J. Lindner, Chemiker-Zeitung 109 (1985) 77.
[43] G. Fritz, G. Becker, G. Poppenbu, M. Rocholl, G. Trenczec, Angew. Chem. Int. Ed. 5 (1966) 53.
[44] W.W. duMont, L.P. Muller, L. Muller, S. Vollbrecht, A. Zanin, J. Organomet. Chem. 521 (1996) 417.
[45] R.A. Benkeser, K.M. Foley, J.B. Grutzner, W.E. Smith, J. Am. Chem. Soc. 92 (1970) 697.
[46] R.A. Benkeser, Acc. Chem. Res. 4 (1971) 94.
[47] C.Q. Nguyen, A. Adeogun, M. Afzaal, M.A. Malik, P. O'Brien, Chem. Commun. (2006) 2179.
[48] C.Q. Nguyen, M. Afzaal, M.A. Malik, M. Helliwell, J. Raftery, P. O'Brien, J. Organomet. Chem., in press.
[49] C.Q. Nguyen, A. Adeogun, M. Afzaal, M.A. Malik, P. O'Brien, Chem. Commun. (2006) 2182.
[50] B. Ludolph, M.A. Malik, P. O'Brien, N. Revaprasadu, Chem. Commun. 17 (1998) 1849.
[51] M. Chuggaze, J. McAleese, P. O'Brien, D.J. Otway, Chem. Commun. 7 (1998) 833.
[52] N. Revaprasadu, M.A. Malik, P. O'Brien, M.M. Zulu, G. Wakefield, J. Mater. Chem. 8 (1998) 1885.
[53] D.J. Crouch, P. O'Brien, M.A. Malik, P.J. Skabara, S.P. Wright, Chem. Commun. 9 (2003) 1454.
[54] T. Trindade, P. O'Brien, X. Zhang, M. Motevalli, J. Mater. Chem. 7 (1997) 1011.
[55] M. Green, P. O'Brien, Chem. Commun. (1998) 2459.
[56] M. Green, P. O'Brien, J. Mater. Chem. 9 (1999) 243.
[57] N. Revaprasadu, M.A. Malik, J. Carstens, P. O'Brien, J. Mater. Chem. 9 (1999) 2885.
[58] M.A. Malik, P. O'Brien, N. Revaprasadu, Adv. Mater. 11 (1999) 1441.
[59] J. McAleese, P. O'Brien, D.J. Otway, Mater. Res. Soc. Symp. Proc. 485 (1998) 157.
[60] C.N.R. Rao, G.U. Kulkarni, V.V. Agrawal, U.K. Gautam, M. Ghosh, U. Tumkurkar, J. Colloid Interface Sci. 289 (2005) 305.
[61] D. Fan, P.J. Thomas, P. O'Brien, J. Mat. Chem. 17 (2007) 1381.
[62] M. Afzaal, M.A. Malik, P. O'Brien, Chem. Commun. 3 (2004) 334.
[63] S.S. Garje, J.S. Ritch, D.J. Eisler, M. Afzaal, P. O'Brien, T. Chivers, J. Mater. Chem. 16 (2006) 966.
[64] C.Q. Nguyen, M. Afzaal, M.A. Malik, P. O'Brien, unpublished results.
[65] C.C. Landry, J. Lockwood, A.R. Barron, Chem. Mater. 7 (1995) 699.